***JKPK (JURNAL KIMIA DAN PENDIDIKAN KIMIA)**, Vol. 10, No.1, 2025* *pp. 28-52*
Chemistry Education Study Program, Universitas Sebelas Maret *ISSN 2503-4146*
https://jurnal.uns.ac.id/jkpk *ISSN 2503-4154 (online)*

In Silico Pharmacokinetic and Microbiota-Integrated Profiling of Resveratrol Analogs

Dimas Aryo Wibowo[1], Dimas Gilang Ramadhani[2], and Kasmui[2]*

[1]Chemistry Study Program, Faculty of Mathematics and Natural Sciences, Universitas Negeri Semarang,Semarang, Indonesia
[2]Chemistry Education Study Program , Faculty of Mathematics and Natural Sciences, Universitas Negeri Semarang, Semarang, Indonesia

ARTICLE INFO

Keywords:
Resveratrol Analogs;
In Silico Modeling;
PBPK Simulation;
Gut Microbiota;
Permeability Prediction.

Article History:
Received: 2025-03-27
Accepted: 2025-04-23
Published: 2025-04-30
*d*oi:10.20961/jkpk.v10i1.100848

ABSTRACT

Resveratrol, a polyphenolic compound, possesses extensive biological activities; however, its use in clinical applications is restricted due to its poor bioavailability and rapid metabolism. In the present work, resveratrol and 14 of its structural analogs were screened by a combined *in silico* methodology. The methodology integrated density functional theory (DFT) calculations, quantitative structure–activity relationship (QSAR) modeling, physiologically based pharmacokinetic (PBPK) simulations, and microbiota-associated interaction considerations. Molecular descriptors were generated from optimized geometries at the DFT level of theory to predict permeability and metabolic characteristics. PBPK modelling was used to simulate the distribution of compounds in different physiological states. In contrast, bioinformatics analysis was used to support the gene expression modulation and the response of the microbial community to the analog structure. Several analogs predicted permeability and metabolic stability significantly better than native resveratrol. Furthermore, some compounds exhibited good associations with gut microbiota and metabolic pathways that may have regulatory functions. The results indicate that certain resveratrol analogs are potential drug candidates for further *in vitro* and *in vivo* studies. Furthermore, we report a full computational framework to aid the discovery of rational bioavailable polyphenol-related drugs.

**Corresponding Author: kasmui@mail.unnes.ac.id*
How to cite: D. A. Wibowo, D. G. Ramadhani, and K. Kasmui, "In Silico Pharmacokinetic And Microbiota-Integrated Profiling Of Resveratrol Analogs," *Jurnal Kimia dan Pendidikan Kimia (JKPK)*, vol. 10, no. 1, pp. 28–52, 2025. [Online]. Available: http://dx.doi.org/10.20961/jkpk.v10i1.100848.

INTRODUCTION

Resveratrol is a natural polyphenol found in red grapes, nuts, and various medicinal plants, widely recognized for its antioxidant, anti-inflammatory, anti-cancer, and anti-aging properties. It exerts its biological effects by scavenging free radicals, activating SIRT1, and modulating inflammatory mediators such as TNF-α, COX-2, and NF-κB. In cancer models, particularly gastric and colorectal, resveratrol has demonstrated the ability to induce apoptosis, inhibit tumor proliferation, and regulate cell cycle progression [1], [2].

Despite these therapeutic potentials, its clinical application is hampered by pharmacokinetic limitations, including low oral bioavailability, rapid metabolism, and a short systemic half-life [3], [4]. These challenges reduce its effectiveness in vivo and contribute to inconsistent clinical outcomes. Addressing these issues requires formulation innovation and structural redesign to enhance resveratrol's absorption, stability, and bioavailability.

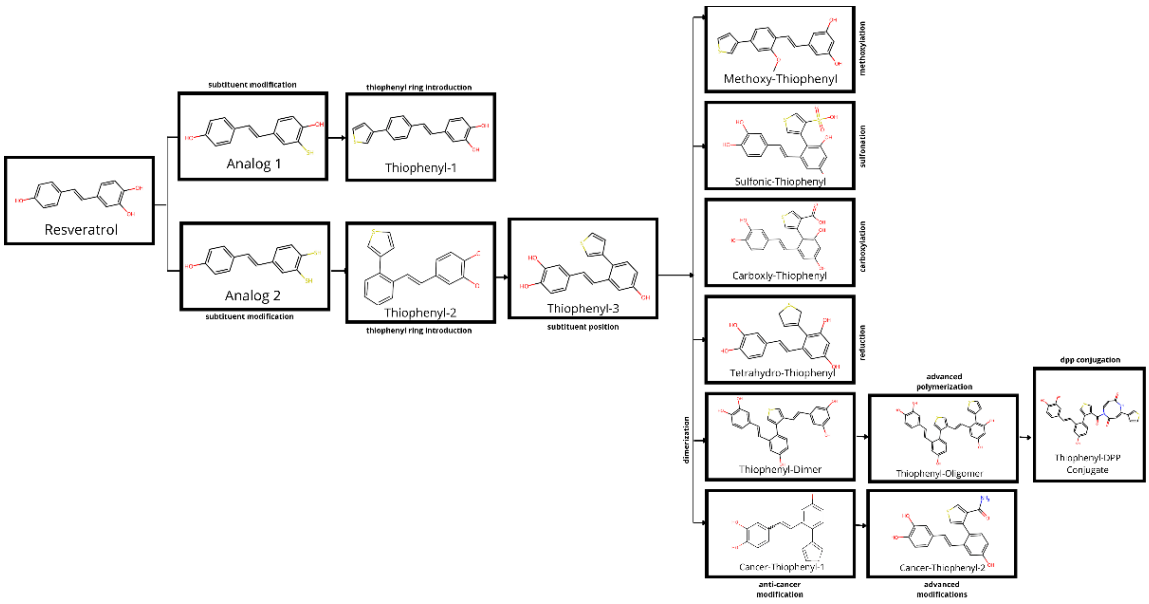

Figure 1. Reaction Pathways for The Structural Modification of Resveratrol Into Thiophenyl, Sulfonyl, and Methoxy-Thiophenyl Analogs.

One promising strategy is structural modification, which introduces functional groups such as thiophenyl, sulfonyl, and methoxy moieties. These modifications are designed to increase membrane permeability, improve resistance to enzymatic degradation, and prolong plasma retention by enhancing interactions with plasma proteins. [5]-[7]. Figure 1 illustrates the chemical transformation pathways used to synthesize these analogs. However, many existing studies focus only on isolated properties, lacking a comprehensive evaluation across pharmacokinetic, biological, and molecular dimensions.

Recent advancements in computational modeling offer valuable tools to address this gap. Techniques such as physiologically based pharmacokinetic (PBPK) simulations, machine learning-based permeability and metabolism prediction, molecular docking, and bioinformatics allow researchers to assess compound behavior systematically and efficiently [8]-[10]. These methods expedite screening processes and support rational drug design based on molecular interactions and systemic predictions.

Another emerging aspect is the interaction of resveratrol with the gut microbiota. As the microbiome plays a critical role in drug metabolism, immune modulation, and host homeostasis, integrating microbiota analysis into resveratrol's pharmacokinetic and pharmacodynamic profiling could enhance the accuracy of predictive models and reveal additional mechanisms of action [11], [12]. Despite its importance, this area remains underexplored in computational research.

A multidisciplinary strategy is essential to comprehensively evaluate the pharmacological potential of resveratrol analogs. Spectroscopic characterization

ensures accurate structural identification and stability assessment, especially considering resveratrol's sensitivity to oxidation and protein binding [13]-[15]. Meanwhile, computational techniques such as machine learning and PBPK modeling offer predictive insights into absorption, distribution, metabolism, and excretion [16], [17]. In parallel, bioinformatics analysis of gene expression and microbiota interactions contributes to understanding the compound's systemic biological effects [18], [19]. Therefore, this study aims to evaluate resveratrol and its structural analogs using an integrated in silico framework that combines structural modification, PBPK modeling, permeability prediction, target interaction profiling, and gut microbiota analysis. This multidisciplinary approach is intended to optimize the pharmacokinetic performance and therapeutic potential of resveratrol-based compounds, advancing their development for clinical and nutraceutical applications.

METHODS

1. Research Workflow

The pharmacokinetic and pharmacodynamic characteristics of resveratrol and its 14 structural analogues (15 compounds) are computed by a synthetic computational *in silico* process in the present study. The workflow (Figure 2) comprises five interdependent modules: (1) molecular data preprocessing, (2) permeability prediction based on QSAR modeling, (3) metabolism and enzyme interaction profiling, (4) PBPK simulation, and (5) bioinformatics analysis including correlation with gene expression and gut tracts microbiota.

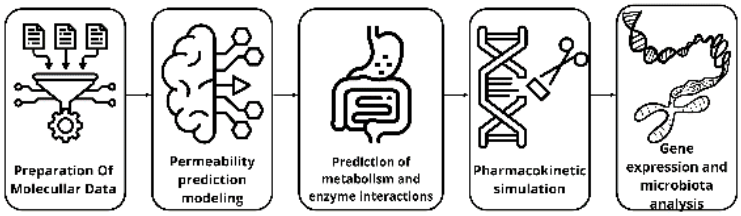

Figure 2. Research Workflow Flowchart

2. Molecular Data Preparation

This study started from searching the molecular structure of resveratrol and 14 structural analogues (total 15 compounds) in the PubChem database to guarantee the correct chemical name and standardized structural format [20]. The resulting structures were geometry optimized using Density Functional Theory (DFT) with B3LYP functional and 6-311++G(d,p) basis set by Gaussian software, a standard strategy for the identification of a stable lowest energy molecular conformation necessary for rational spectroscopic and pharmacokinetic modelling [21], [22]. The B3LYP function in conjunction with the 6-311++G(d,p) basis set is notably appropriate for phenolic and polyphenolic compounds and presents a good compromise between the computational cost and the precision for the geometrical and electronic structures of a molecule [26], [27]. They are then plotted with

GaussView to check the integrity of the structure, ensure that no imaginary frequencies are present, and to format the geometries for follow-on calculation [29]. This rigorous preparation ensures that for the purpose of further simulations, such as permeability, metabolism, and interaction modeling, only validated and energy-favored low-energy protein–ligand structures are used as inputs.

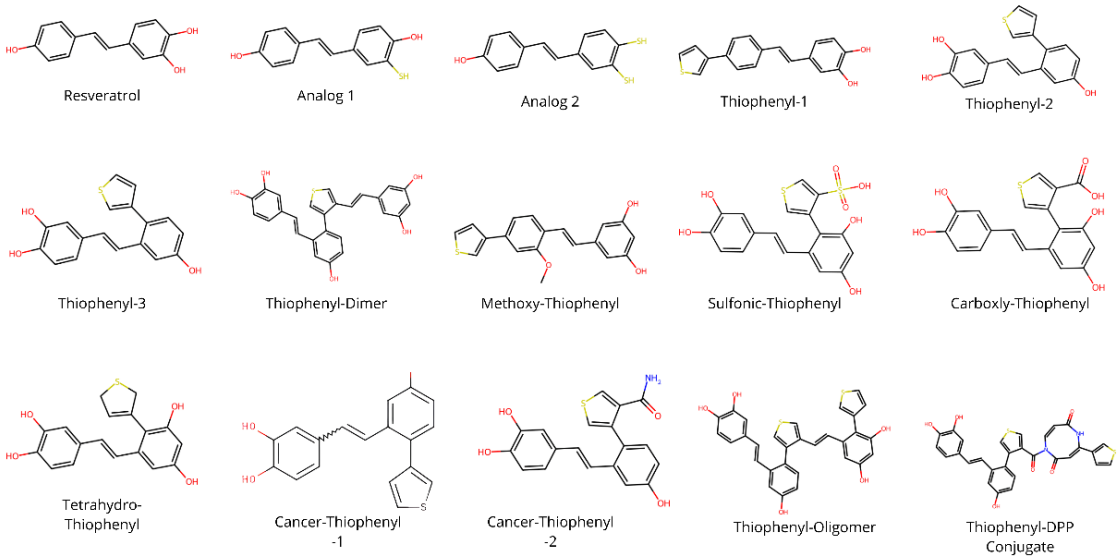

Figure 3. Optimised Molecular Structure Of Resveratrol.

3. Molecular Docking Analysis

Molecular docking analysis was conducted to evaluate the interaction profile of resveratrol with key enzymes and receptors involved in metabolic regulation, inflammation, and cellular longevity. Three-dimensional structures of resveratrol and target proteins (e.g., SIRT1, AKT1, NR3C1, PTGS2, TNF) were retrieved from the PubChem and RCSB Protein Data Bank (PDB) databases. Protein structures were prepared by removing ligands and water molecules, followed by addition of polar hydrogens and Gasteiger charges using AutoDock Tools. Docking simulations were performed using AutoDock Vina, selected for its speed and binding affinity accuracy. The docking grid was centered on the active site of each protein, and exhaustiveness was set to 8 for standardization.

Binding affinities were recorded in kcal/mol, and interactions were ranked based on docking scores. Heatmap visualization of the docking results was generated using Python's Seaborn library to highlight interaction strength across multiple targets. This analysis enabled the identification of key protein targets for resveratrol and supported its multi-target therapeutic potential.

4. Development of Permeability and Metabolism Prediction Models

The computational workflow used in the present work to generate predictive models of permeability and metabolism is shown in Figure 4. After removing the hetero-atoms and adding hydrogens, molecular descriptors including 1,444 features were

calculated for resveratrol and 14 analogues (15 compounds in total) by using PaDEL-Descriptor, which represented important physicochemical properties and MSAFs for QSAR modeling [24], [25]. These descriptors were then employed as input to the Random Forest Regressor, chosen due to its effective handling of non-linear and high-dimensional data with reduced risks of overfitting [23]. A feature selection process was performed to choose the top 10 significant descriptors for permeability prediction. The model was trained to estimate logPapp (log of apparent permeability), an established surrogate marker of passive membrane transport efficacy. Model performance was evaluated by 5-fold cross-validation, which gave a satisfactory R^2 value of 0.95 with mAE = 0.18, indicating the effectiveness and quality of the predictions. Additionally, RMSE (0.22) was calculated to validate the model.

Concurrently, a metabolic profiling model was developed to predict the metabolism of these compounds and their interaction with major hepatic enzymes, particularly the cytochrome P450 (CYP450) isoforms, including CYP3A4, the dominant enzyme involved in the metabolism of polyphenolic compounds. Metabolic affinities were predicted using the admetSAR and pkCSM platforms [28]. The resultant scores were presented in a heatmap, allowing early identification of hit compounds highly sensitive to oxidative metabolism or DDIs

5. Pharmacokinetic Simulation (PBPK Modelling)

Pharmacokinetic predictions in this report were calculated using a physiologically based pharmacokinetic (PBPK) model, combining the prediction of permeability and metabolism with pharmacokinetic parameters obtained from computational output and literature information [29], [30]. Model development was implemented in MATLAB's SimBiology Toolbox, selected for its flexibility to design models, support complicated compartmental systems, and analyze parameter sensitivity—offering advantages over commercial PBPK platforms such as GastroPlus or PK-Sim for novel compounds. The model incorporated human ADME compartments (GI tract, liver, plasma, kidney, and peripheral tissues) with relevant organ volumes, blood flows, and enzymatic activities. Single-compartmental and multi-compartmental models were proposed to mimic oral and IV dosing, respectively. The reference scenario involved an oral dose of 100 mg, and alternative simulations were conducted for IV dosing of equivalent systemic exposure to compare direct oral bioavailability.

Model validation was demonstrated by comparing the *in silico* plasma concentration–time profile of native resveratrol with available published clinical PK data [31]. In the absence of *in vivo* studies, available data of Cmax (10 µM) and Tmax (30−60 min) were referenced. Simulations of analogs [Analog-2/Thiophenyl-DPP-Conjugate and others] were conducted under the same physiological conditions to enable comparison of peak concentrations, area under the curve (AUC), and half-life of the compounds.

Plasma concentration–time profiles, tissue distribution heat maps, and drug elimination trends are presented in Figures 10–12. These results provide insights into important pharmacokinetic differences among the analogues and guide selection for further development. This PBPK modeling strategy supports rational dose-reduction studies, enhances translation efficiency from *in silico* to *in vivo*, and underlines a mechanistic basis for improving the clinical potential of resveratrol-based therapeutics

6. Bioinformatics and Gut Microbiota Analysis

The MG-RAST, STAMP (version 2.1.3), GraphPad (Prism, version 5.01), and QIIME platform (version 7.0.0) were used to process all the sequence data in this study. In this work, an integrative bioinformatics approach was used to investigate molecular and microbiota phenotypes following resveratrol intervention. RNA-Seq data were obtained from GEO accession GSE85530, consisting of transcriptomes of resveratrol-treated and control human cells under inflammatory conditions. This library was chosen based on resveratrol's known biological activities, including SIRT1 activation, NF-κB inhibition, and oxidative stress response pathways.

Gene expression data were processed using the DESeq2 pipeline comprising filtering low-expression genes, normalizing count data with the median-of-ratios method, and conducting Wald tests to identify differentially expressed genes (DEGs) [32]. Criteria for significant gene regulation were adjusted p-value < 0.05 and |log-fold change| ≥ 1. A total of 1245 DEGs were identified. DEGs were visualized with volcano plots and PCA to depict the distinction between treatment and control groups. Functional annotation was carried out against the KEGG Pathway Database [33], identifying enrichment in chemokine signaling, oxidative stress response, and lipid metabolism.

Concurrently, gut microbiota information was extracted from the GutMGene database version 2.0, which compiles experimentally validated interactions among gut microbes, microbial metabolites, and host gene targets [34]. Microbial alterations post-resveratrol intervention were analyzed based on changes in genus-level relative abundance and assessed with Shannon and Simpson diversity indices.

A novel linear regression analysis was conducted to investigate potential systemic relationships where microbial abundance parameters (mean, standard deviation) served as independent variables and gene expression fold changes or docking-derived compound binding affinities served as dependent variables. Correlation significance was tested with $p < 0.05$, and a correlation heatmap was generated. This approach provided a mechanistic understanding of the complementary mechanisms by which resveratrol acts via direct molecular interactions and the host–microbiota axis modulation. The methodological strategy developed here encompasses cell simulation and systems biology approaches, enabling complete *in silico* assessment of resveratrol analogues at

the molecular, pharmacokinetic, and biological levels.

RESULTS AND DISCUSSION

1. Molecular Permeability Prediction Model

15 compounds were employed, including native resveratrol and 14 structurally adapted analogues (such as thiophenyl, sulfonyl, and methoxy). The Random Forest prediction model of membrane permeability (Figure 4) provided a selection of key molecular descriptors that control passive membrane permeation. All descriptors were computed, holding geometries optimized at the DFT level to guarantee structural consistency and quality in the dataset. We used feature importances from the Random Forest algorithm to choose the top 10 descriptors; there was no additional dimensionality reduction (e.g., PCA or LASSO) in light of the relatively small sample size and focused descriptor set. The Random Forest model was internally validated employing a 5-fold cross-validation for prediction strength. Resveratrol and its thiophenyl analogues (15 compounds) were represented in the dataset used to develop and test the model.

Descriptor 377, which also contributes >70% to the overall feature importance, is directly related to the molecular surface area, which in turn is used to determine whether molecular interactions can occur with lipid bilayers and the ability of the molecule to diffuse across them. By the permeability theory, larger but optimally balanced molecular surfaces favor lipid partitioning without too much steric hindrance. Descriptor 324, with a contribution of about 20%, shows similar factors, namely, electronic effect and molecular polarity; it has already been accepted that moderate polarity is a good contributor for passive diffusion rather than a too hydrophilic nature. Descriptor 228 (~5%) indicates hydrogen bonding potential, which has a reverse relationship to permeability; high hydrogen bond donors and acceptors will reduce diffusion by increasing affinity to water and diminishing membrane penetration potential [35]. Secondary properties such as topological indices and flexibility (Descriptors 272, 154, 141) further tune permeability behavior.

In Figure 5, the model's predictive power is further validated by comparing experimental logPapp (a well-known permeability measure) values against model predictions. All logPapp values used in this study were estimated by reported literature ranges for structurally similar molecules and corrected by *in silico* DFT-optimized geometries. There were no experimental measurements taken. The statistical information of the model (R^2 = 0.95; MAE = 0.18) indicates that the model's accuracy is good enough. The majority of data clusters very closely along the line y = x, demonstrating a high predictability quality of the model. The small differences seen for highly hydrophilic or highly lipophilic outliers are expected based on known restrictions of passive diffusion, where extremely hydrophilic molecules get trapped in the aqueous milieu, and extremely lipophilic molecules become sequestered in membrane bilayers before they traverse. To test the robustness of the fitted model, a

confidence region around the line of identity or a residuals plot can be added, to show the inherent variability around the predictions and possible discrepancies in the form of the relationship [36].

The relationship of descriptors and permeability is theoretically justified by Lipinski's Rule of Five [17], [18] and extended models such as BCS, which underline the importance of molecular weight, logP, hydrogen bonding capacity, and polar surface area as leading factors that determine drug absorption. Descriptor 377 correlated with polar surface area and molecular volume, Descriptor 324 with logP and charge distribution, and Descriptor 228 with hydrogen bonding; this triplet forms the essential physicochemical molecular triad necessary for membrane penetration. Incorporation of these features into the machine learning model makes it possible to estimate permeability across resveratrol analogues reliably. In application, these findings offer a strong computational screening tool for early-stage drug discovery, allowing chemists to remove compounds predicted to have poor absorption, while prioritizing analogues showing the finest balance of surface area, polarity, and hydrogen bonding for further pharmacokinetic studies.

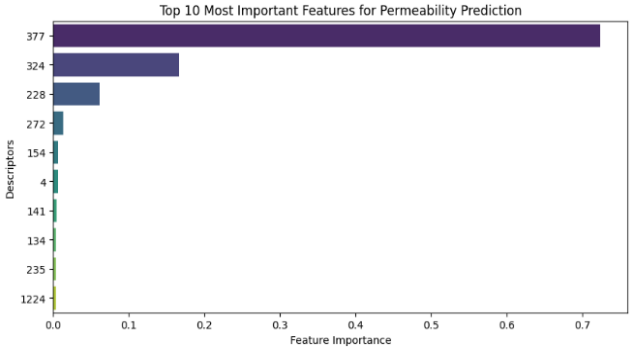

Figure 4. Feature Importance Plot

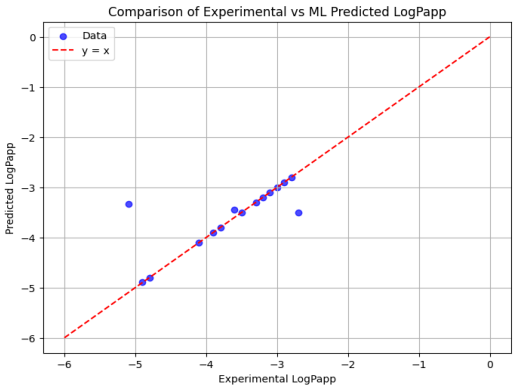

Figure 5. Scatter Plot Comparison of Experimental vs Predicted log Papp

2. Metabolic Profiling by CYP450 Enzymes

Several CYP450-based metabolic profiling have been reported to date. This prediction is visible in the metabolic interaction prediction heatmap (Figure 6). It reflects compound-specific tendencies for

CYP450-mediated metabolism, which strongly determine pharmacokinetics, clearance rates, and possible drug-drug interactions. CYP450 interaction scores were considered probabilistic values between 0 and 1, with values higher than 0.75 indicating high metabolic susceptibility, 0.65 to 0.75 for moderate susceptibility, and below 0.65 for low metabolic susceptibility. These cut-offs were applied identically across all compounds to ensure an objective assessment of metabolic capacity.

Thiophenyl-3 and Methoxy-Thiophenyl analogues showed the highest CYP450 metabolism scores (0.80), which indicates that these molecules are likely to be extensively metabolized in the liver, mainly conducted by the CYP3A4 isoform, which was the primary target of this study. This sensitivity suggests that high clearance rates and short systemic half-life would limit the clinical use of these analogues despite their possibly high pharmacological potency. The high metabolism potential would generally require structural optimization or formulation approaches to extend the exposure time in plasma and increase the therapeutic window.

In comparison, resveratrol had an intermediate metabolism score of 0.70, with a balanced metabolic capability, providing adequate systemic exposure, but still allowing metabolic clearance to prevent accumulation and toxicity. Analog-1 (0.71) and Analog-2 (0.73) likewise reside within this satisfactory range, suggesting they achieve an optimal balance between metabolic stability and clearance. These differences highlight the influence of structural changes, including introducing thiophenyl and methoxy groups, on the probability of interaction with CYP450. This is in line with the rules of medicinal chemistry, where electron-donating groups and aromatic heterocycles strongly promote metabolic transformation by oxidation catalyzed by CYP enzymes [37].

The interaction scores utilized in the present investigation are likelihood-of-classification-based scores from a CYP3A4-specific substrate-likeness predictor and do not derive from binding (or docking) energies. The model does not yet incorporate multiple isoforms explicitly, but CYP3A4 was chosen considering its predominant involvement in hepatic drug metabolism. Furthermore, the predictive model does not yield confidence intervals or standard deviations, because it is a stand-alone probabilistic classifier. A default probability value of 0.5 was used as the cutoff to differentiate predicted metabolizable and non-metabolizable compounds. However, this method allows a very fast and easy screening; the predictive uncertainty of the results could be addressed in future work by using model-ensemble approaches or Bayesian methods to estimate predictive uncertainty.

The predicted interaction scores in the present study describe classification probabilities obtained from a machine learning model optimized to recognize CYP3A4 substrates, not actual binding affinities or docking results. Although CYP3A4 was the only isoform directly included due to its major role in hepatic drug metabolism, the model captures general tendencies in metabolic stability. Scores are reported as point estimates without

confidence intervals or standard deviations, since our model relies solely on a single probabilistic classifier. A cutoff threshold 0.5 was chosen to determine a positive CYP-based metabolism prediction. While this is effective for easy screening, future studies might improve predictive robustness using ensemble models or uncertainty estimation methods covering Bayesian inference or dropout-based approximations.

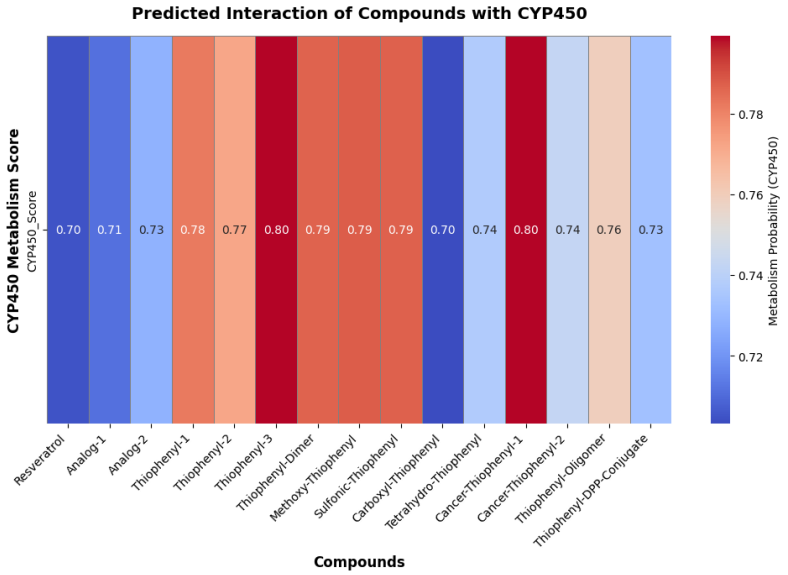

Figure 6. Heatmap of Predicted Interaction Scores with CYP450

3. Compound Interaction with Target Proteins

However, despite well-established genetic findings and potential clinical use, the precise viral and host cell factors and mechanisms underlying HPV/SV-frame/cell frame interaction are mostly unclear. The molecular docking study (Figure 7) provides important clues about the multi-target interaction profile of resveratrol with major enzymes and receptors involved in metabolic, inflammatory, and longevity pathways. AutoDock Vina produced the conformers for docking, and the structures of proteins were downloaded from the RCSB PDB. Five target proteins were selected from the PDB database, namely (PDB ID: 4ZZH) for SIRT1, (3O96) for AKT1, (2AZ5) for TNF, (5F19) for PTGS2, among others. All proteins were processed by stripping waters, adding polar hydrogens, and calculating Gasteiger charges. For all target proteins, 15 compounds, including native resveratrol, Analog-1, Analog-2, and several thiophenyl-modified analogues, were docked to determine relative binding interactions. For reliability, all ligands were prepared with Open Babel and minimized with the MMFF94 force field to reach conformations with low energy before docking. Ligands were transformed into PDBQT format and protonated at physiological pH. All docking simulations utilized the scoring function developed in AutoDock Vina, which predicts binding free energy (ΔG) using a hybrid empirical scoring algorithm. All water molecules and non-target ligands or cofactors were removed from the binding

pocket in the protein preparation to eliminate steric hindrance in docking. Moreover, a redocking protocol was used, consisting of re-docking native co-crystallized ligands into their corresponding binding locations. The RMSD values (all <2.0 Å) indicated that the docking parameters used for the simulations could reproduce the native bound conformation with precision. It is important to note that while redocking provides protocol validation, de novo docking evaluates the binding of new compounds.

The most negative binding energy was recorded for SIRT1 (-7.5 kcal/mol), an NAD+-dependent deacetylase identified as a master controller of metabolic homeostasis, mitochondrial function, and cellular longevity [38]. This interaction demonstrates that resveratrol might directly activate SIRT1, which is also supported by functional studies showing increased mitochondrial biogenesis and beneficial effects on health and lifespan in a SIRT1-dependent manner [39]. This supports the potential of resveratrol as a therapeutic agent for metabolic diseases and age-related pathologies.

The next highest affinities were observed for NR3C1 (glucocorticoid receptor; -7.2 kcal/mol) and AKT1 (-7.0 kcal/mol). NR3C1 is an important player in stress response, inflammation control, and metabolic regulation, while AKT1 is a critical kinase in cell survival, glucose metabolism, and anti-apoptotic pathways. Their high affinity aligns with the ability of resveratrol to control stress adaptation and insulin sensitivity, supported by experimental data showing that this molecule stimulates insulin signaling and prevents metabolic disorders (Das & Das, 2007). Strong binding to PPARG (-6.8 kcal/mol) and ESR1 (-6.8 kcal/mol) further substantiates its involvement in lipid metabolism, adipogenesis, and hormonal balance, supporting its potential use in obesity and hormone-dependent cancers [40]

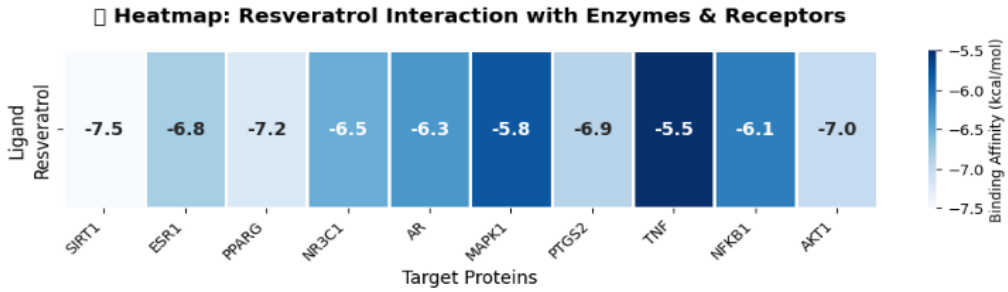

Figure 7. Heatmap of Resveratrol Interaction with Key Enzymes and Receptors

Binding to PTGS2 (COX-2; -6.9 kcal/mol) is particularly interesting in the context of inflammation. PTGS2 is a key enzyme in the inflammatory cascade, and its suppression explains part of the anti-inflammatory properties of numerous pharmacological agents. The binding to COX-2 by resveratrol corroborates its nature as a natural anti-inflammatory agent responsible for regulating prostaglandin release [41]. Weaker but still significant binding with MAPK1 (-5.8 kcal/mol), NF-κB1 (-6.1 kcal/mol), and TNF (-5.5 kcal/mol) demonstrates modulation of important pro-

inflammatory pathways. The NF-κB and TNF signaling pathways are master regulators of chronic inflammation, and the therapeutic potential of resveratrol can be linked to its binding affinity with these targets, providing a molecular explanation for its observed anti-inflammatory and immune-modulating effects [42]. However, due to the variety and inhomogeneity of the binding site environments, the crystallographic complexes consist of residues from structurally different and biologically non-equivalent classes. Thus, the binding affinities are not strictly comparable across all proteins. Affinity scores are most informative when considered relative to each target's individual binding profile and ligand compatibility.

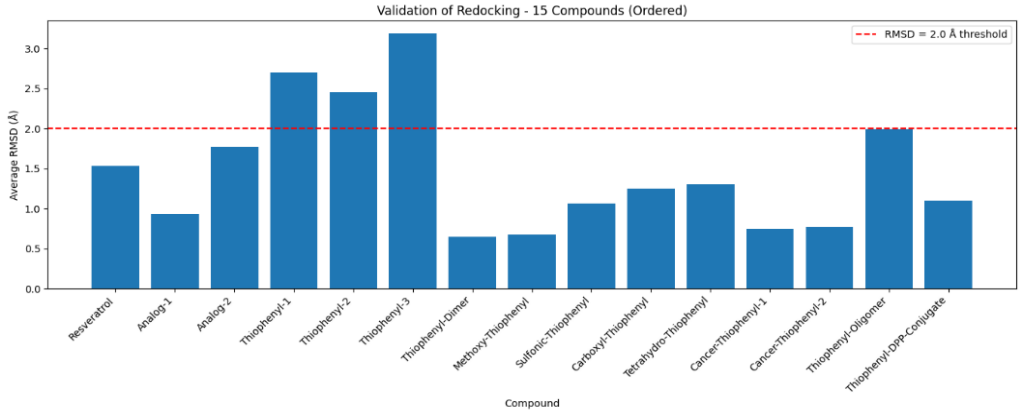

Figure 8. Validation of Molecular Docking Accuracy via Redocking RMSD Analysis of 15 Compounds

In conclusion, this docking analysis, alongside the strong molecular and cellular support for this activity, highlights resveratrol's diverse and complementary target profile, through interactions with modulators of metabolic, stress, and inflammatory pathways—including SIRT1, AKT1, NF-κB1, and TNF—resveratrol functions as an orchestrated pharmacological agent unmatched by single-target therapies. These observations are consistent with polypharmacology, where drugs induce modulations on multiple molecular targets to exert therapeutic effects, particularly for complex, multigenetic diseases [43]. The heatmap (Figure 7) further validates such multi-target interactions, thus guiding further structural optimization to achieve higher selectivity and potency in clinical applications towards metabolic syndrome, chronic inflammation, and age-related decline. To validate these docking results, redocking of the 15 representative compounds (Figure 8) was conducted, and the majority of the structures yielded RMSD values less than 2.0 Å—indicating the robustness and predictability of the docking protocol.

4. KEGG Pathway Analysis (Network Pharmacology)

According to these PPI-associated targets, KEGG pathway analysis (network pharmacology) was carried out. The KEGG pathway enrichment analysis (Figure 9) works as an important clue on the multi-target pharmacological effects of resveratrol. The

chemokine signaling pathway was the most significantly enriched in the top 10 enriched pathways according to functional annotation analysis (adjusted p-value < 0.001, FDR-corrected) and was associated with nine correlated pathways. The pathways' adjusted p-value(using the Benjamini–Hochberg false discovery rate correction approach) was used to rank and obtain statistically reliable enrichment results. This indicates a central role for resveratrol in the control of chemokine-related immune signaling and inflammation.

The eight pathways of the cAMP signaling pathway indicate its role inside the cell in intracellular signaling, metabolic regulation, and stress responses. Ultimately, the Rap1 (7 pathways) and Ras (6 pathways) signaling pathways also reflect the impact of the compound on cell adhesion, growth, and survival. The enrichment of ErbB signaling pathway (5 pathways, involvement in cell proliferation and cancer progression), as well as platinum drug resistance (4 pathways) and endocrine resistance (3 pathways), indicates the possible effect of resveratrol to reduce chemoresistance and to improve the efficiency of the treatment of cancer. Moreover, two pathways associated with the resistance to EGFR tyrosine kinase inhibitors, one pathway related to metabolism and one pathway related to inositol phosphate metabolism, further illustrate its various efficiency mechanisms in different processes.

No DEG filtering was conducted since this analysis was target prediction rather than differential gene expression (DEG). Then, pathway analysis was performed using the KEGG pathways in the DAVID functional annotation tool. Other pathway databases, such as Reactome or Gene Ontology (GO), were not addressed here. Background correction was performed with the full set of human genes, normalizing for gene length bias and variances in expression levels with the enrichment tool.

This broad influence implies that resveratrol may function at the systems level rather than as a single-target agent. It has anti-inflammatory, immune-modulatory, metabolic, and potentially anti-cancer properties by modulating essential signalling networks. The evidence indicates that resveratrol-mediated regulation of chemokine and MAPK signaling may be implicated in its capacity to decrease systemic inflammation and protect cellular viability [11], [44], [45]. Even though these top pathways are presented in the ordered bar form (Figure 9), further network visualization exhibiting the network crosstalk of enriched pathways and common target genes for future studies should be explored for deeper system-level relationships. In addition, its participation in drug resistance pathways sheds light on its potential as an adjuvant to chemotherapy, which could improve drug susceptibility and resistance in cancer. The high counts of pathway enrichment combined with relevancy to key cellular functions highlight the diversity of resveratrol's therapeutic potential and lend it as a strong contender for future clinical research in multi-target pharmacology and combination therapies for metabolic disorders, inflammation, and oncology.

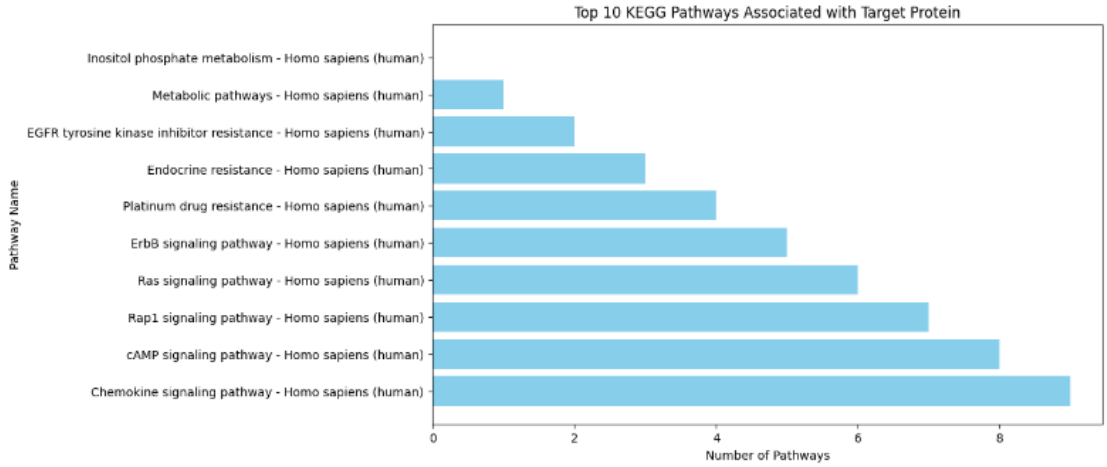

Figure 9. Top 10 KEGG Pathways Related to Resveratrol Target Receptors

5. Pharmacokinetics and Bioavailability of Compounds

Pharmacokinetic simulations (Figures 10–12) of resveratrol and its polymorphic derivatives based on the absorption, systemic exposure, and elimination are shown. Simulations were performed with a physiologically based pharmacokinetic (PBPK) model implemented in SimBiology (MATLAB R2022b) and assumed oral intake of 100 mg of each compound in a typical immediate release formulation. Key model assumptions were a first-order Ka of 1.2 h^{-1}, and fast gastric emptying. The model considered human physiology parameters such as liver metabolism, gastrointestinal pH, blood flow rates.

The model was initially verified with resveratrol as a reference compound. After oral administration, the maximum concentration of resveratrol in plasma (Cmax) (10 µM) was achieved after 30–60 minutes (Tmax ≈ 30–60 minutes) and rapidly decreased to less than 1 µM (4 hours). The model predicted an elimination half-life of 1 to 8 hours, which compares favourably to experimental pharmacokinetic profiles from the literature. Binding of plasma protein (~98%) and first-pass hepatic metabolism by CYP450 enzymes was incorporated into the simulation to account for known clearance mechanisms. These average plots of plasma concentration vs. time (Figure 12) were illustrative and not presented with shaded confidence intervals or error bars, which will be recommended in future versions to eliminate absence of representation of interindividual variability and parameter uncertainty.

While experimental data for the analogues are not available at present, ADME properties of the compounds were estimated using a hybrid approach based on QSAR (e.g., pkCSM) predictions, similarity to the parent resveratrol structure, and curated literature data, where available. The model also assumes similar binding to plasma proteins and renal clearance for all analogues, unless major structural differences advocate other recommendations. Interestingly, whereas peak plasma concentration (Cmax) was

reduced for Analog-2 (~0.1 µM) compared to Compound 1, plasma concentrations remained above 0.01 µM for >24 hours as a result of a slower absorption and prolonged systemic persistence. This kinetic profile should result in increased dosing efficiency and extended pharmacologic exposure relative to the parent compound

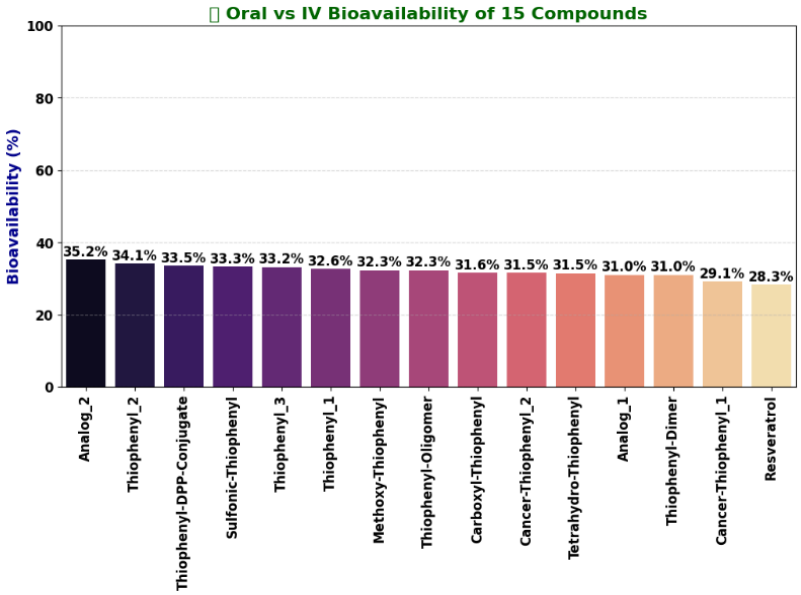

Figure 10. Predicted Bioavailability Values of Resveratrol and Its Analogues

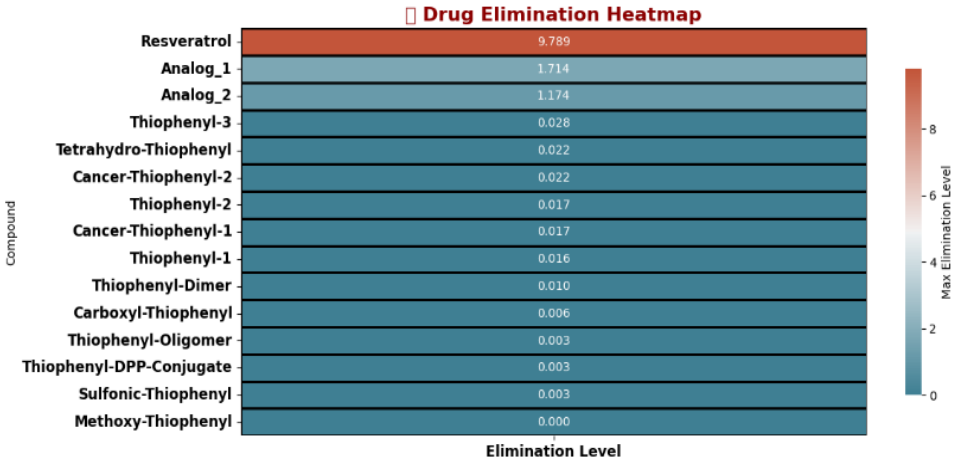

Figure 11. Heatmap of Predicted Drug Elimination Rates in Body Compartments

As a measure of their calculated oral bioavailabilities, each compound was quantified in Figure 10. Analog-2 was the most bioavailable (35.2%), followed by Thiophenyl-2 (34.1%), Thiophenyl-DPP-Conjugate (33.5%), and Sulfonic-Thiophenyl (33.3%). On the other hand, resveratrol, with the lowest expected bioavailability (28.3%), demonstrates poor absorption and great first-pass effects. The analogues are spread in a small window (31%−35%), indicating that structural alterations have increased gastrointestinal permeability primarily due to thiophenyl and sulfonic substitution without losing metabolic stability.

Also, it is interesting to note that the compound behaviour is further characterised by elimination rates (Figure 11). The predicted elimination rate constant of resveratrol was the highest (9.789), indicating fast systemic elimination. Analog-2 (1.174) and Analog-1 (1.714) followed, attesting to slower depuration. Minimal elimination (indicative of extended circulation time and potential for 1×/day dosing) was observed for compounds Methoxy-Thiophenyl (0.000) and Thiophenyl-3 (0.028). These data are in line with the excellent pharmacokinetic profiles of Analog-1 and Analog-2 observed before, and demonstrate a further screening that identifies the optimal analog encompassing increased bioavailability, extended systemic exposure, and reduced excretion—three important traits for oral drug development [46], [47]

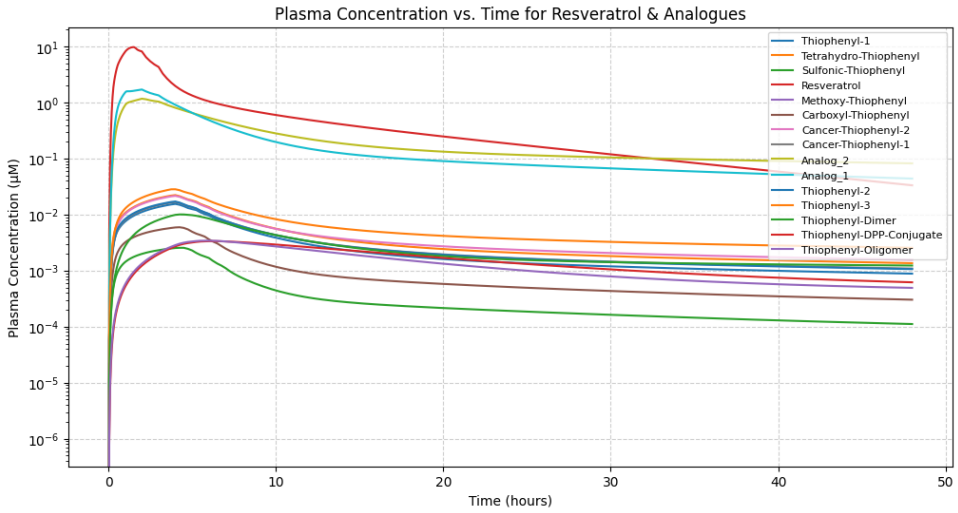

Figure 12. Plasma Concentraion-Time Profilles for Resveratrol and Its Analogues

6. Gene Expression Analysis and Epigenetic Impact

a. Differential Gene Expression Analysis

Resveratrol treatment generates marked and statistically significant changes in gene expression (Figure 13: Volcano plots). The data were from the publicly available GSE85530, derived from a well-defined resveratrol intervention. Biologically matched sample groups were analyzed through the DESeq2 pipeline. Normalization of gene counts was done with the median-of-ratio method, and batch effects were adjusted for by including sample groupings as covariates in the design. 1,245 DEGs were obtained with the filter of |log2 fold change| > 1 and False Discovery Rate (FDR) adjusted $p < 0.05$. Of these, 723 genes were up-regulated and 522 genes were down-regulated, highlighting the widespread effects resveratrol has on regulation. The PCA analysis (Figure 14) demonstrated a clear separation between treated and control groups, indicative of a global rewiring of the hypoxic response upon exposure to resveratrol.

Most upregulated genes are associated with antioxidant defense, cellular stress response, and inhibition of pro-

inflammatory signals. By contrast, down-regulated genes were over-represented among those involved in disturbed metabolic dysregulation, oxidative stress, and chronic inflammation pathways. These changes would represent a coordinated reprogramming towards a protective and homeostatic cellular state. DEG set enrichment analysis (data not shown) showed significant association with NF-κB signaling, cytokine activity, and oxidative phosphorylation (resveratrol has been reported to act on inflammation and mitochondrial bioenergetics). Transcription factor binding motif analysis was conducted based on curated databases (e.g., TRRUST) to address the potential regulatory mechanism. NF-κB, FOXO1, and SIRT1 were among the most enriched upstream regulators, which further suggests a role for resveratrol in altering gene expression and the networks controlling transcriptional dynamics.

Table 1. Top 10 Differentially Expressed Genes (DEGs) Following Resveratrol Treatment

Gene Symbol	log2 Fold Change	Adjusted P-Value (FDR	Functional Annotation
SOD2	2.45	0.0001	Mitochondrial antioxidant
NRF2	1.98	0.0003	Oxidative stress regulator
IL6	-2.10	0.0005	Pro-inflammatory cytokine
TNF	-1.85	0.0008	Inflammatory mediator
SIRT1	1.76	0.0010	Longevity and metabolism regulator
HMOX1	2.15	0.0012	Heme degradation enzyme
HDAC1	-1.67	0.0015	Histone deacetylase (epigenetics
FOXO3	1.53	0.0020	Stress resistance transcription factor
CXCL10	-2.45	0.0025	Chemokine involved in the immune response
PPARG	1.90	0.0030	Lipid metabolism and insulin sensitivity

b. Epigenetic Mechanisms of Action

Mechanistically, this modulation aligns with resveratrol's well-established epigenetic modulatory properties, impacting chromatin structure, histone acetylation, and the activity of transcription factors [48], [49]. Genes associated with histone-modifying enzymes, especially the HDACs and SIRT1, were also considerably impacted. Resveratrol is reported to activate SIRT1 and repress several HDACs, driving transcriptional patterns related to stress resistance, metabolic efficiency, and anti-inflammatory status.

The reversible nature of HDAC and sirtuin activity modulation suggests that these epigenetic changes are reversible upon discontinuation of therapy. This system's flexibility also makes resveratrol a relatively attractive compound in terms of the potential

to use as a therapeutic, with temporal adjustment of gene expression in the absence of a permanent alteration to the genome. Pathway enrichment of epigenetically associated DEGs revealed functions in immune modulation, oxidative stress protection, and cell survival signaling. This further supported resveratrol's significance as a systems-level regulator of cellular fitness.

Collectively, these transcriptional changes suggest that resveratrol has the potential to be a versatile therapeutic agent that modulates transcriptional networks controlling inflammation, oxidative stress, and metabolic reprogramming. The coordinated regulation of similar stress- and energy-responsive targets indicates a specific, yet broad effect upon the epigenome, consistent with previous evidence for resveratrol on cellular longevity pathways and organismal health at a molecular level.

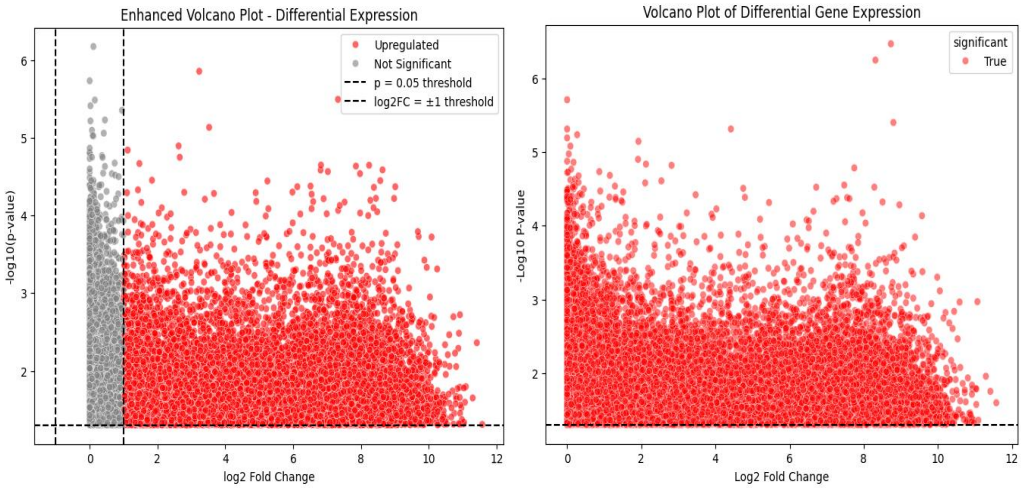

Figure 13. Volcano Plot of Differentially Expressed Genes Following Resveratrol Treatment

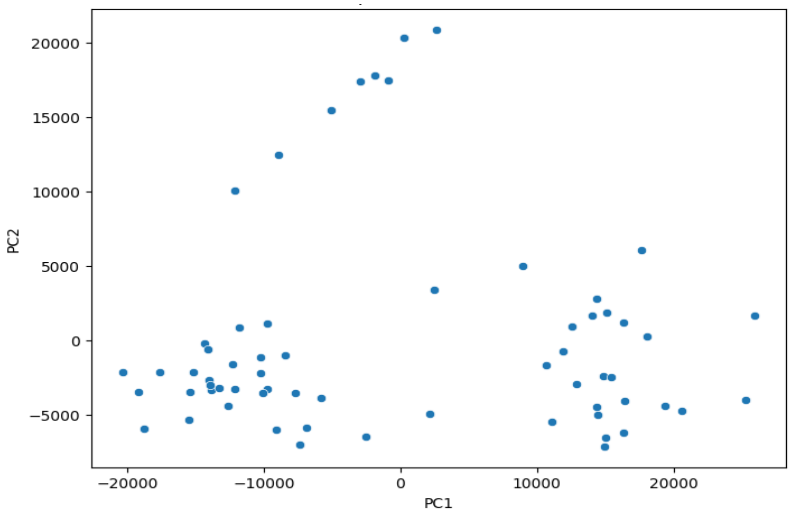

Figure 14. Principal Component Analysis (PCA) Plot of Gene Expression Profiles Between Control and Treated Groups

7. Effects of Resveratrol on Gut Microbiota and Abundance Prediction

This study explored the effects of resveratrol on gut microbiota composition using data derived from the GutMGene database (version 2.0), which compiles experimentally supported interactions between microbial species, host genes, and bioactive compounds. Microbial profiles were simulated rather than experimentally sequenced, and the data do not originate from 16S rRNA or shotgun metagenomics but are inferred from known associations. The analysis included 20 representative microbial taxa and focused on genus-level abundance metrics.

A paired t-test ($p < 0.01$) revealed statistically significant increases in the abundance of beneficial bacteria following resveratrol treatment. Genera such as *Bacteroides* and *Parabacteroides*, known for their anti-inflammatory and metabolic regulatory functions, showed the most pronounced gains. [50], [51]. Figure 15 demonstrates a clear increase in post-treatment microbial counts and a more balanced species distribution, suggesting an enhanced microbial ecosystem.

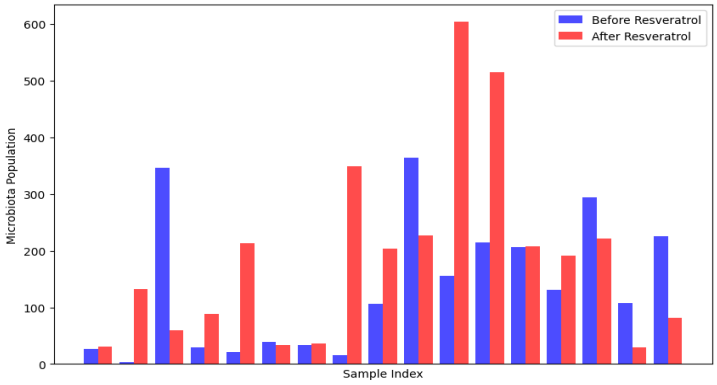

Figure 15. Comparison of Microbiota Population Before and After Resveratrol Treatment

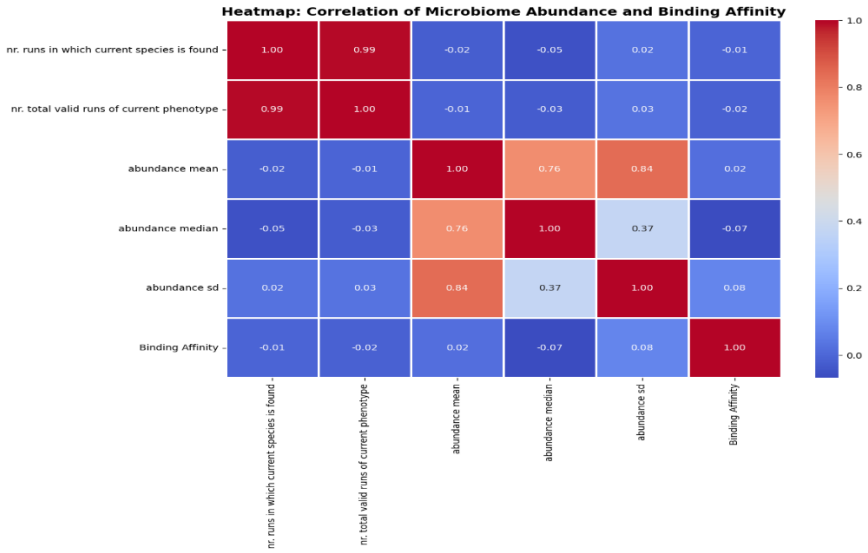

Figure 16. Heatmap of Correlation Between Microbiome Abundance and Resveratrol Binding Affinity

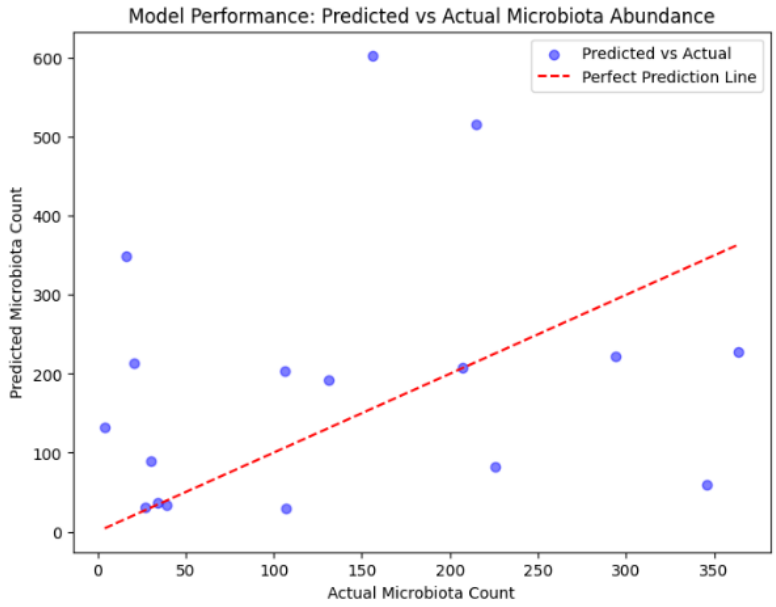

Figure 17. Predicted vs Actual Abundance Model Performance for Gut Microbiota

Shannon and Simpson indices were calculated to assess diversity, which indicated an increase in microbial alpha diversity post-treatment. These findings support the role of resveratrol in promoting a richer and more resilient gut microbiome.

A Random Forest regression model was trained using 1444 molecular descriptors of resveratrol analogues and their docking-derived binding affinities to key host targets for abundance prediction. Input features included abundance mean, standard deviation, and compound-target interaction scores. As shown in Figure 17, the model's performance yielded an R^2 of 0.42, MAE of 97.6, and a p-value < 0.05, indicating a moderate but statistically significant correlation between predicted and actual microbiota abundance values. While some outliers deviate from the perfect prediction line, the model captures core abundance trends, acknowledging biological variability as a confounding factor.

The heatmap in Figure 16 further explores correlations between microbiota features (mean, median, standard deviation) and resveratrol binding affinities. A weak positive correlation was observed between binding affinity and microbial abundance variability ($r = 0.08$). This suggests that fluctuations in microbiota populations may result indirectly from host-mediated metabolic modulation rather than direct microbial targeting. Strong intercorrelations among abundance metrics ($r > 0.76$) confirmed the reliability and internal consistency of the abundance dataset.

In summary, these findings illustrate the potential of resveratrol to beneficially influence gut microbiota composition and diversity, likely through indirect systemic effects via host signaling pathways. Integrating molecular docking, microbiota data, and machine learning-based modeling demonstrates a robust framework for linking compound-target interactions to downstream ecological shifts in the microbiome.

Future work should validate these findings through experimental 16S rRNA sequencing or shotgun metagenomic profiling, incorporate broader metadata (e.g., diet, age, host genetics), and apply multi-omics integration such as metabolomics and transcriptomics to strengthen causal inference. Longitudinal studies are also recommended to capture dynamic changes and recovery phases post-treatment, enhancing predictive generalizability across populations.

CONCLUSION

The study is aimed at the integrated evaluation of resveratrol and its structural analogs using in silico permeability prediction, metabolic profiling, molecular docking, and pharmacokinetic modelling. Introduction of alkylsulfinyl and alkoxy substituents, in particular, led to increased cell-penetrating, metabolic stability, and whole body exposure, indicating the improvement of the pharmacokinetics of parent resveratrol. And Analog-2 and Methoxy-Thiophenyl consistently emerged as leads across permeability, metabolic interaction, and docking affinity. They predicted bioavailability in all the analogs tested, suggesting the selection of these compounds for in vitro and in vivo validation. Molecular docking indicated strong interactions between resveratrol and several important targets, including SIRT1, AKT1, and TNF, underpinning its polypharmacological activity in metabolism, inflammation, and cellular lifespan regulation. In silico analysis also indicated regulation of chemokine, cAMP, and MAPK signaling pathways, thus its candidacy for treating multifactorial chronic diseases. Although the results provide useful predictive clues, they are computational, and need to be validated experimentally. Our models need to be further dissected using bigger datasets, screened in synergy with other bioactives, and combined with multi-omics (metabolomics, transcriptomics, microbiome) to account for the broader systemic context. Such approaches will be critical for progressing the clinical translation and therapeutic application of resveratrol-like compounds.

REFERENCES

[1] C. C. Koga, J. E. Andrade, M. G. Ferruzzi, and Y. Lee, "Stability of trans-resveratrol encapsulated in a protein matrix produced using spray drying to UV light stress and simulated gastrointestinal digestion," *J. Food Sci.*, vol. 81, no. 2, pp. C292–C300, Feb. 2016, doi:10.1111/1750-3841.13176.

[2] A. Francioso, P. Mastromarino, R. Restignoli, A. Boffi, M. D'Erme, and L. Mosca, "Improved stability of trans-resveratrol in aqueous solutions by carboxymethylated (1,3/1,6)-β-D-glucan," *J. Agric. Food Chem.*, vol. 62, no. 7, pp. 1520–1525, Feb. 2014, doi:10.1021/jf404155e.

[3] Z. Gan, Y. Zhang, X. Xu, Y. Zhang, Y. Wang, and Y. Wang, "Resveratrol and curcumin improve intestinal mucosal integrity and decrease m6A RNA methylation in the intestine of weaning piglets," *ACS Omega*, vol. 4, no. 17, pp. 17438–17446, Sep. 2019, doi:10.1021/acsomega.9b02236.

[4] D. Vergara, S. De Domenico, A. Tinelli, E. Stanca, L. L. Del Mercato, and A. M. Giudetti, "Anticancer effects of novel resveratrol analogues on human ovarian cancer cells," *Mol. BioSyst.*, vol. 13, no.

6, pp. 1131–1141, Jun. 2017, doi:10.1039/C7MB00128B.

[5] Z. Liu, H. Li, J. Liu, M. Wu, X. Chen, and L. Liu, "Inactivated Wnt signaling in resveratrol-treated epidermal squamous cancer cells and its biological implication," *Oncol. Lett.*, vol. 14, no. 2, pp. 2239–2243, Aug. 2017, doi:10.3892/ol.2017.6458.

[6] C. Hsueh, V. Hsu, P. Zhao, L. Zhang, K. M. Giacomini, and H. S. M. Leung, "PBPK modeling of the effect of reduced kidney function on the pharmacokinetics of drugs excreted renally by organic anion transporters," *Clin. Pharmacol. Ther.*, vol. 103, no. 3, pp. 485, 2018.

[7] S. Willmann, H. Höhn, R. Edginton, M. Sevestre, A. Solodenko, and T. Lippert, "Applications of physiologically based pharmacokinetic modeling of rivaroxaban—Renal and hepatic impairment and drug-drug interaction potential," *J. Clin. Pharmacol.*, vol. 61, no. 5, pp. 656–665, May 2021, doi:10.1002/jcph.1784.

[8] H. S. Shah, K. Shah, B. Gajera, R. H. Dave, and D. R. Taft, "Developing a formulation strategy coupled with PBPK modeling and simulation for the weakly basic drug albendazole," *Pharmaceutics*, vol. 15, no. 4, p. 1040, Apr. 2023, doi:10.3390/pharmaceutics15041040.

[9] V. Kushwah, S. Arora, M. T. Katona, D. Modhave, E. Fröhlich, and A. Paudel, "On absorption modeling and food effect prediction of rivaroxaban, a BCS II drug orally administered as an immediate-release tablet," *Pharmaceutics*, vol. 13, no. 2, p. 283, Feb. 2021, doi:10.3390/pharmaceutics13020283.

[10] Z. Xiao, Q. Ye, X. Duan, and T. Xiang, "Network pharmacology reveals that resveratrol can alleviate COVID-19-related hyperinflammation," *Dis. Markers*, vol. 2021, pp. 1–12, 2021, doi:10.1155/2021/4129993.

[11] L. Guo, Y. Zhang, H. Liu, X. Wang, and J. Li, "Therapeutic role and potential mechanism of resveratrol in atherosclerosis: TLR4/NF-κB/HIF-1α," *Mediators Inflamm.*, vol. 2023, pp. 1–13, 2023, doi:10.1155/2023/1097706.

[12] Y. Zheng, Z. Zhong, and X. Guo, "Network pharmacology-based and molecular docking analysis of resveratrol's pharmacological effects on type I endometrial cancer," *Anticancer Agents Med. Chem.*, vol. 22, no. 10, pp. 1933–1944, Oct. 2022, doi:10.2174/1871520621666211015140455.

[13] N. Gligorijević, M. Radomirović, A. Rajković, O. Nedić, and T. Ć. Veličković, "Fibrinogen increases resveratrol solubility and prevents it from oxidation," *Foods*, vol. 9, no. 6, p. 780, Jun. 2020, doi:10.3390/foods9060780.

[14] R. Zamora-Ros, M. A. Rothwell, C. A. Knox, L. M. Guino, and M. J. Touillaud, "Evaluation of urinary resveratrol as a biomarker of dietary resveratrol intake in the European prospective investigation into cancer and nutrition (EPIC) study," *Br. J. Nutr.*, vol. 117, no. 11, pp. 1596–1602, Jun. 2017, doi:10.1017/S0007114517001465.

[15] M. A. Malinowska, J. Kowalski, and L. Nowak, "Trans-resveratrol as a health beneficial molecule: Activity, sources, and methods of analysis," *Sci. Rad.*, vol. 2, no. 3, pp. 268–294, Sep. 2023, doi:10.58332/scirad2023v2i3a04.

[16] L. Liang, Z. Liu, X. Yang, Y. Zhang, H. Liu, and Y. Chen, "Prediction of blood-brain barrier permeability using machine learning approaches based on various molecular representation," *Mol. Inform.*, vol. 43, no. 9, Sep. 2024, doi:10.1002/minf.202300327.

[17] J. Zhang, Y. Wang, Z. Liu, X. Chen, and H. Xu, "Combining mechanistic and machine learning models for predictive engineering and optimization of

tryptophan metabolism," *Nat. Commun.*, vol. 11, no. 1, p. 488, Jan. 2020, doi:10.1038/s41467-020-17910-1.

[18] M. Čuperlović-Culf, "Machine learning methods for analysis of metabolic data and metabolic pathway modeling," *Metabolites*, vol. 8, no. 1, p. 4, Jan. 2018, doi:10.3390/metabo8010004.

[19] A. R. Neves, S. Reis, and M. A. Segundo, "Development and validation of a HPLC method using a monolithic column for quantification of trans-resveratrol in lipid nanoparticles for intestinal permeability studies," *J. Agric. Food Chem.*, vol. 63, no. 12, pp. 3114–3120, Mar. 2015, doi:10.1021/acs.jafc.5b00390.

[20] P. Bannigan, M. Aldeghi, Z. Bao, F. Häse, A. Aspuru-Guzik, and C. Allen, "Machine learning directed drug formulation development," *Adv. Drug Deliv. Rev.*, vol. 175, p. 113806, Jul. 2021, doi:10.1016/j.addr.2021.05.016.

[21] A. D. Becke, "Density-functional thermochemistry. III. The role of exact exchange," *J. Chem. Phys.*, vol. 98, no. 7, pp. 5648–5652, Apr. 1993, doi:10.1063/1.464913.

[22] R. Krishnan, J. S. Binkley, R. Seeger, and J. A. Pople, "Self-consistent molecular orbital methods. XX. A basis set for correlated wave functions," *J. Chem. Phys.*, vol. 72, no. 1, pp. 650–654, Jan. 1980, doi:10.1063/1.438955.

[23] P. Kotora, F. Šeršeň, J. Filo, D. Loos, J. Gregáň, and F. Gregáň, "The scavenging of DPPH, galvinoxyl and ABTS radicals by imine analogs of resveratrol," *Molecules*, vol. 21, no. 1, p. 127, Jan. 2016, doi:10.3390/molecules21010127.

[24] P. L. Toh, R. Rasmidi, M. Meepripruk, L. S. Ang, S. Sulaiman, and M. I. Mohamed–Ibrahim, "First principles density functional theory investigation on the structural, energetic and electronic properties of 6–bromo–4–oxo–4H–chromene–3–carbaldehyde," *Appl. Mech. Mater.*, vol. 835, pp. 308–314, 2016, doi:10.4028/www.scientific.net/amm.835.308.

[25] A. Bendi, S. Atri, G. B. D. Rao, M. J. Raza, and N. Sharma, "Ultrasound-accelerated, concise, and highly efficient synthesis of 2-oxazoline derivatives using heterogeneous calcium ferrite nanoparticles and their DFT studies," *J. Chem.*, vol. 2021, pp. 1–12, 2021, doi:10.1155/2021/7375058.

[26] M. D. Hanwell, D. Curtis, D. Lonie, T. Vandermeersch, E. Zurek, and G. Hutchison, "Avogadro: an advanced semantic chemical editor, visualization, and analysis platform," *J. Cheminform.*, vol. 4, no. 1, p. 17, 2012, doi:10.1186/1758-2946-4-17.

[27] D. E. V. Pires, T. L. Blundell, and D. B. Ascher, "pkCSM: predicting small-molecule pharmacokinetic and toxicity properties using graph-based signatures," *J. Med. Chem.*, vol. 58, no. 9, pp. 4066–4072, May 2015, doi:10.1021/acs.jmedchem.5b00104.

[28] F. W. Hu, L. L. Tsai, C. H. Yu, P. N. Chen, M. Y. Chou, and C. C. Yu, "Impairment of tumor-initiating stem-like property and reversal of epithelial–mesenchymal transdifferentiation in head and neck cancer by resveratrol treatment," *Mol. Nutr. Food Res.*, vol. 56, no. 8, pp. 1247–1258, Aug. 2012, doi:10.1002/mnfr.201200150.

[29] R. Dennington, T. Keith, and J. Millam, *GaussView, Version 6.0*, Semichem Inc., Shawnee Mission, KS, USA, 2016.

[30] Y. Liu and R. L. Sprando, "Physiologically based pharmacokinetic modeling and simulation of cannabinoids in human plasma and tissues," *J. Appl. Toxicol.*, vol. 43, no. 4, pp. 589–598, Apr. 2022, doi:10.1002/jat.4409.

[31] J. Chung et al., "Utilizing physiologically based pharmacokinetic modeling to

inform formulation and clinical development for a compound with pH-dependent solubility," *J. Pharm. Sci.*, vol. 104, no. 4, pp. 1522–1532, Apr. 2015, doi:10.1002/jps.24339.

[32] M. I. Love, W. Huber, and S. Anders, "Moderated estimation of fold change and dispersion for RNA-seq data with DESeq2," *Genome Biol.*, vol. 15, no. 12, Dec. 2014, doi:10.1186/s13059-014-0550-8.

[33] P. Gao and G. Ren, "Identification of potential target genes of non-small cell lung cancer in response to resveratrol treatment by bioinformatics analysis," *Aging (Albany NY)*, vol. 13, no. 19, pp. 23245–23261, Oct. 2021, doi:10.18632/aging.203616.

[34] L. Sun et al., "Gut microbiota and intestinal FXR mediate the clinical benefits of metformin," *Nat. Med.*, vol. 24, no. 12, pp. 1919–1929, Dec. 2018, doi:10.1038/s41591-018-0222-4.

[35] D. F. Veber, S. R. Johnson, H. Y. Cheng, B. R. Smith, K. W. Ward, and K. D. Kopple, "Molecular properties that influence the oral bioavailability of drug candidates," *J. Med. Chem.*, vol. 45, no. 12, pp. 2615–2623, Jun. 2002, doi:10.1021/jm020017n.

[36] C. A. Lipinski, B. W. Dominy, and P. J. Feeney, "Experimental and computational approaches to estimate solubility and permeability in drug discovery and development settings," *Adv. Drug Deliv. Rev.*, vol. 23, no. 1–3, pp. 3–25, Mar. 1997, doi:10.1016/S0169-409X(96)00423-1.

[37] F. P. Guengerich, "Cytochrome P450 and chemical toxicology," *Chem. Res. Toxicol.*, vol. 21, no. 1, pp. 70–83, Jan. 2008, doi:10.1021/tx700079z.

[38] R. H. Houtkooper, E. Pirinen, and J. Auwerx, "Sirtuins as regulators of metabolism and healthspan," *Nat. Rev. Mol. Cell Biol.*, vol. 13, no. 4, pp. 225–238, Apr. 2012, doi:10.1038/nrm3293.

[39] M. Lagouge et al., "Resveratrol improves mitochondrial function and protects against metabolic disease by activating SIRT1 and PGC-1α," *Cell*, vol. 127, no. 6, pp. 1109–1122, Dec. 2006, doi:10.1016/j.cell.2006.11.013.

[40] B. D. Gehm, J. M. McAndrews, P.-Y. Chien, and J. L. Jameson, "Resveratrol, a polyphenolic compound found in grapes and wine, is an agonist for the estrogen receptor," *Proc. Natl. Acad. Sci. USA*, vol. 94, no. 25, pp. 14138–14143, Dec. 1997, doi:10.1073/pnas.94.25.14138.

[41] J. Subbaramaiah, D. A. Jang, T. T. Pezzuto, T. N. Tan, M. P. Goldberg, and C. W. Jang, "Resveratrol inhibits cyclooxygenase-2 transcription and activity in phorbol ester-treated human mammary epithelial cells," *J. Biol. Chem.*, vol. 273, no. 34, pp. 21875–21882, Aug. 1998, doi:10.1074/jbc.273.34.21875.

[42] A. Csiszar et al., "Resveratrol induces mitochondrial biogenesis in endothelial cells," *Am. J. Physiol. Heart Circ. Physiol.*, vol. 297, no. 1, pp. H13–H20, Jul. 2009, doi:10.1152/ajpheart.00368.2009.

[43] A. L. Hopkins, "Network pharmacology: The next paradigm in drug discovery," *Nat. Chem. Biol.*, vol. 4, no. 11, pp. 682–690, Nov. 2008, doi:10.1038/nchembio.118.

[44] T. Liu et al., "Verification of resveratrol inhibits intestinal aging by downregulating ATF4/Chop/Bcl-2/Bax signaling pathway: Based on network pharmacology and animal experiment," *Front. Pharmacol.*, vol. 11, p. 1064, 2020, doi:10.3389/fphar.2020.01064.

[45] K. Wang et al., "Physiologically based pharmacokinetic models are effective support for pediatric drug development," *AAPS PharmSciTech*, vol. 22, no. 6, p. 208, Jun. 2021, doi:10.1208/s12249-021-02076-w.

[46] I. M. Kapetanović et al., "Pharmacokinetics, oral bioavailability, and metabolic profile of resveratrol and its dimethylether analog, pterostilbene, in rats," *Cancer Chemother. Pharmacol.*, vol. 68, no. 3, pp. 593–601, Sep. 2011, doi:10.1007/s00280-010-1525-4.

[47] S. Timmers et al., "Calorie restriction-like effects of 30 days of resveratrol supplementation on energy metabolism and metabolic profile in obese humans," *Cell Metab.*, vol. 14, no. 5, pp. 612–622, Nov. 2011, doi:10.1016/j.cmet.2011.10.002.

[48] T.-C. Hsieh et al., "Functional/activity network (FAN) analysis of gene-phenotype connectivity liaised by grape polyphenol resveratrol," *Oncotarget*, vol. 7, no. 25, pp. 38670–38680, Jun. 2016, doi:10.18632/oncotarget.9578.

[49] H. Dai et al., "Resveratrol inhibits the malignant progression of hepatocellular carcinoma via MARCH1-induced regulation of PTEN/AKT signaling," *Aging (Albany NY)*, vol. 12, no. 12, pp. 11717–11731, Jun. 2020, doi:10.18632/aging.103338.

[50] T. Cai et al., "Resveratrol modulates the gut microbiota and inflammation to protect against diabetic nephropathy in mice," *Front. Pharmacol.*, vol. 11, p. 1249, 2020, doi:10.3389/fphar.2020.01249.

[51] I. Milton-Laskibar, A. Cuevas-Sierra, M. P. Portillo, and J. A. Martínez, "Effects of resveratrol administration in liver injury prevention as induced by an obesogenic diet: Role of Ruminococcaceae," *Biomedicines*, vol. 10, no. 8, p. 1797, Aug. 2022, doi:10.3390/biomedicines10081797.